AGU PUBLICATIONS

Journal of Advances in Modeling Earth Systems

RESEARCH ARTICLE
10.1002/2017MS001025

Analysis of near-surface biases in ERA-Interim over the Canadian Prairies

Alan K. Betts[1] and **Anton C. M. Beljaars**[2]

[1]Atmospheric Research, Pittsford, Vermont, USA, [2]ECMWF, Reading, UK

Key Points:
- We quantify the biases in the diurnal cycle of temperature in ERA-Interim as a function of opaque cloud cover using hourly data from Canadian Prairie stations
- The biases are largest in the warm season, and they change from spring to fall
- The biases have a different structure in the cold season with surface snow cover

Correspondence to:
A. K. Betts,
akbetts@aol.com

Citation:
Betts, A. K., and A. C. M. Beljaars (2017), Analysis of near-surface biases in ERA-Interim over the Canadian Prairies, *J. Adv. Model. Earth Syst.*, *9*, 2158–2173, doi:10.1002/2017MS001025.

Received 20 APR 2017
Accepted 29 AUG 2017
Accepted article online 31 AUG 2017
Published online 13 SEP 2017

Abstract We quantify the biases in the diurnal cycle of temperature in ERA-Interim for both warm and cold season using hourly climate station data for four stations in Saskatchewan from 1979 to 2006. The warm season biases increase as opaque cloud cover decreases, and change substantially from April to October. The bias in mean temperature increases almost monotonically from small negative values in April to small positive values in the fall. Under clear skies, the bias in maximum temperature is of the order of −1°C in June and July, and −2°C in spring and fall; while the bias in minimum temperature increases almost monotonically from +1°C in spring to +2.5°C in October. The bias in the diurnal temperature range falls under clear skies from −2.5°C in spring to −5°C in fall. The cold season biases with surface snow have a different structure. The biases in maximum, mean and minimum temperature with a stable BL reach +1°C, +2.6°C and +3°C respectively in January under clear skies. The cold season bias in diurnal range increases from about −1.8°C in the fall to positive values in March. These diurnal biases in 2 m temperature and their seasonal trends are consistent with a high bias in both the diurnal and seasonal amplitude of the model ground heat flux, and a warm season daytime bias resulting from the model fixed leaf area index. Our results can be used as bias corrections in agricultural modeling that use these reanalysis data, and also as a framework for understanding model biases.

Plain Language Summary Global model forecasts and analyses of temperature are used for many purposes, including agriculture, where accuracy is needed to estimate crop growth. This paper uses long term temperature records from climate stations in Saskatchewan on the Canadian Prairies to show how the biases in the maximum and minimum temperature in a European Weather Centre reanalysis vary with season and cloud cover; so that these biases can be corrected.

1. Introduction

A series of papers have analyzed the coupling of the seasonal and diurnal climatology of the Canadian Prairies to land-surface properties, such as snow cover and agriculture cropping, as well as to reflective cloud cover [*Betts et al.*, 2013a, 2013b, 2014a, 2014b, 2015, 2016, 2017; *Betts and Tawfik*, 2016] using hourly climate data from 15 stations in the Canadian Prairies. These hourly climate data provide a solid observational basis for understanding land surface coupling for this region; so now we ask whether they can be used to improve the representation of clouds and land-surface processes in atmospheric models. Society depends on models for forecasting the weather on weekly and monthly timescales, as well global model simulations to understand our changing global climate.

At Agriculture and Agri-Food Canada, soil-plant-climate models are used to predict crop production and soil carbon change as well as nitrous oxide emissions for present and future climate change scenarios [*Smith et al.*, 2009, 2013]. These models are also used to evaluate the impact of management practices and to assess the sustainability of agricultural practices [*Desjardins et al.*, 2001, 2005]. All of these models require some type of weather or climate data as input in order to drive the mechanisms that estimate planting and harvest dates, crop growth and production; as well as organic matter decomposition, nutrient losses and trace gas emissions. The complexity of weather/climate data required as input varies from relatively simple estimates of daily minimum and maximum temperature, to more complex variables such as hourly solar radiation, cloud cover and relative humidity. Generally, these weather/climate variables are tightly coupled to each other. In order to ensure model performance is maximized, a suite of high-quality weather/climate

© 2017. The Authors.
This is an open access article under the terms of the Creative Commons Attribution-NonCommercial-NoDerivs License, which permits use and distribution in any medium, provided the original work is properly cited, the use is non-commercial and no modifications or adaptations are made.

variables are the preferred input. For an analysis of the past, measured climate data are available as input to the agricultural models. For an analysis of the future, whether seasonal or longer term, all weather/climate data required as input by an agricultural model must be obtained from global circulation models (GCMs). Over time these GCMs used for forecasting weather and climate have improved, but forecast output variables still have biases for specific regions and/or specific times of the year. This is of concern, since GCM weather/climate outputs are currently incorporated into agricultural modeling without accounting for biases, and any bias will affect the modeled agricultural system.

This paper uses the observational results from the Prairie climate papers [*loc. cit*.) to analyze the biases in the near-surface data from the European Centre for Medium-range Weather Forecasts [ECMWF) reanalysis [*Dee et al*., 2011] known as ERA-Interim (which we shall abbreviate as ERAI). It is clear from observational studies that there are large differences in the land-atmosphere-cloud coupling between the warm season without snow and the cold season with surface snow [*Betts et al*., 2013a, 2014a; *Betts and Tawfik*, 2016]. The high reflectivity of snow on the Prairies of the order of 0.7, acts as a climate switch between largely non-overlapping climate states separated by 10K. Without surface snow, the boundary layer [BL) processes are dominated by shortwave cloud forcing with the highest afternoon temperature maximum and deepest unstable BL under clear skies. However with reflective surface snow, long-wave cloud forcing dominates, and under clear skies, temperatures fall giving a strong stable BL. Snow cover also reduces evaporation, and insulates the ground reducing the ground heat flux. Guided by these observational results, we analyze the ERAI biases for the warm season with no snow and the cold season with surface snow separately, and partition our analysis by observed opaque cloud cover. The separate issue of the biases in the length of the snow season in ERAI has been analyzed elsewhere [*Snauffer et al*., 2016].

In earlier studies with the ECMWF model it was shown that the diurnal cycle and particularly the night time cooling is very sensitive to turbulent mixing and to surface to subsurface heat transfer processes. *Viterbo et al*. [1999] reduced winter cooling by introducing the process of soil moisture freezing and by increasing the turbulent mixing in the stable boundary layer. Both mechanisms contributed to the reduction of excessive surface cooling. More recently, after the introduction of ERAI, *Dutra et al*. [2010] reduced the heat diffusion in snow by improving the snow density formulation, resulting in more cooling over Siberia in winter. Repetition of the *Viterbo et al*., [1999] sensitivity experiments has shown that the latest model version responds differently to diffusion parameters than the 1999 model version [*Holtslag et al*., 2013]. The insulation of the snow in the recent model version has decoupled the atmosphere from the subsurface, and has made the winter and night time cooling much more sensitive to atmospheric turbulent diffusion. It is concluded that diurnal cycles can be optimized by atmospheric turbulent diffusion as well as subsurface processes, and parameter optimization may not be unique. In the current study, we identify the error structure in the near-surface temperatures in ERAI across cloud cover and season, and suggest parameters and processes that are candidates for optimization.

2. Land-Surface Model in ERA-Interim

The operational ECMWF analysis-forecast system is under continual development with significant upgrades typically twice a year. For historic reanalysis a frozen version of the model is used. The ERA-Interim reanalysis used model cycle CY31R1, which was introduced operationally in 2006. This reanalysis starts with 1979 and continues to the present. However, our comparison period is 1979–2006, because the climate stations we use have no snow depth observations after 2006.

The atmosphere-surface interaction in reanalysis systems is important for the simulation of near-surface temperatures. ERAI uses the Tiled ECMWF Scheme for Surface Exchanges over Land (TESSEL [*Van den Hurk et al*., 2000]) to represents terrain heterogeneity in a simplified way. For each grid point, it has 6 separate tiles, namely for low vegetation, high vegetation, snow on low vegetation and bare soil, high vegetation with snow beneath, a wet interception reservoir, and bare soil. The distinction between low and high vegetation is particularly important for snow, because exposed snow has a high albedo, whereas a canopy with snow underneath has a low albedo [*Betts and Ball*, 1997; *Betts et al*., 2001]. The vegetation characteristics in ERAI are defined by fractional cover and type of dominant high and low vegetation and are based on the Global Land Cover Characterization [GLCC) data set derived from 1 km AVHRR [Advanced Very High Resolution Radiometer) satellite observations [*Loveland et al*., 2000]. Correspondence tables define parameters like

leaf area index, minimal stomatal resistance, roughness length and rooting profile dependent on vegetation type. Uniform global soil hydraulic properties correspond to a medium texture soil. The snow and interception tiles are dynamic and depend on snow depth and interception water content. Each tile has a skin temperature which represents the radiative surface temperature of the vegetation canopy, the snow surface or the bare soil skin. The vegetation layer is thermally coupled to the underlying soil or snow by an empirical conductivity. More details are given in Part IV, Chapter 7 of the Integrated Forecasting System [IFS] documentation of CY31R1 [*ECMWF*, 2007].

The boundary layer scheme of the IFS provides the turbulent exchange of momentum, heat and moisture between the atmosphere and the surface. The surface layer part is based on Monin-Obukhov similarity with empirical stability functions and vegetation-type dependent roughness lengths for momentum and heat/moisture [*Beljaars and Viterbo*, 1998]. The snow model is a slab model with prognostic variables for snow mass, temperature, albedo and density [*Douville et al*., 1995]. The fractional snow cover increases linearly with snow mass per unit area, and reaches 100% at 15 kg/m^2.

The coupled land-atmosphere model plays an important role in the analysis system because it propagates the state of the atmosphere and land variables in time and provides a background to the analysis. The latter is done for the atmosphere in 12 h cycles with a four-dimensional variational method. The temperature and dewpoint at 2 m are analyzed separately with an optimal interpolation method at 0, 6, 12 and 18 UTC. However, these fields do not affect the atmospheric analysis directly. Instead they are used to infer soil moisture and soil temperature fields [*Douville et al*., 2000]. Snow mass has a separate analysis scheme based on the Cressman method using snow depth observations from surface (SYNOP) stations and snow cover from satellites [*Drusch et al*., 2004].

The focus of this paper is on model biases, and therefore we are not using the analyzed 2m temperature fields. Instead we use only the short-term forecasts from the 0 and 12 UTC analyses at forecast steps of 3, 6, 9, and 12 h, which has the advantage that the diurnal cycle is fairly well resolved. In addition to the 3 hourly values, the forecast model also keeps maximum and minimum temperatures for each 3 h period. The reason for taking the very short range to study model biases is that we would like to be as close as possible to the large scale analysis, so errors can be attributed to the model formulation and uncertainty in land surface variables rather than to errors in the large scale flow. In fact, the short range forecasts used as background for the analyses are often indistinguishable from the analysis, i.e., the increments from observations tend to be small. The latter is characteristic of a good analysis system. The model is capable of representing the large scale meteorology very well and only needs small increments to follow the real synoptic developments. This is not the case for near surface variables that are subject to fast processes and uncertain surface boundary conditions. It is well known from operational verification that systematic errors in near surface variables like 2m temperature and dewpoint (which are not used by the analysis) are already present right from the start of the forecast [e.g., *Haiden et al*., 2016].

3. Data Processing

Our primary comparison uses daily means of temperature (T_m), together with maximum (T_x) and minimum temperature (T_n) and the diurnal range of temperature

$$DTR = T_x - T_n \tag{1}$$

The reduction of the hourly Prairie data to daily means is discussed in *Betts et al*. [2013a] and the reduction of the 3 hourly ERAI data to daily means (and daily T_x and T_n) is discussed in *Betts et al*. [2015]. We define the bias of a variable X as the difference of ERAI from the climate observations

$$\text{bias}: X = X(\text{ERAI}) - X(\text{data}) \tag{2}$$

The Prairie data has proved extremely useful because trained observers recorded hourly an opaque cloud fraction in tenths: defined as clouds that obscured the sun, moon or stars. This was done for cloud layers and for the total sky: we use the total sky fraction. The observers have followed the same protocol for the past 60 years, and there are very few missing hourly observations. Consequently, following our earlier papers, we use these hourly opaque cloud observations to calculate daily means, and use these to stratify the reanalysis biases, which are sensitive to cloud cover. In addition, we use 12 years of high quality

Table 1. Climate Stations With Location and Elevation

Station Name	Station ID	Province	Latitude (°)	Longitude (°)	Elevation (m)
Regina	4016560	Saskatchewan	50.43	−104.67	578
Estevan	4012400	Saskatchewan	49.22	−102.97	581
Prince Albert	4056240	Saskatchewan	53.22	−105.67	428
Saskatoon	4057120	Saskatchewan	52.17	−106.72	504
The Pas	5052880	Manitoba	53.97	−101.1	270

shortwave and longwave radiation data from the baseline surface radiation network (BSRN) station at Bratt's Lake, 25km south of Regina Saskatchewan [*Betts et al.*, 2015] to calculate the ERAI biases of downward shortwave and longwave radiation, stratified with the daily mean opaque cloud from Regina.

4. Dependence of ERAI Daily Biases on Opaque Cloud

4.1. Prairie Warm Season Biases

We merged four stations in Saskatchewan, Estevan, Regina, Saskatoon and Prince Albert, which form a south-north cross section (see Table 1), and compared the warm season data (April to October 1979–2006, for days with no snow cover in either ERAI or the observations) between the climate stations and the nearest grid-point from ERAI. There are a total of 17,927 days. The model grid-points have dominantly low vegetation cover (Table 2).

Figure 1 stratifies T_x, T_m, T_n and DTR using ten bins for the observed daily mean opaque cloud cover (as a fraction). The left panel shows the mean values for observations and reanalysis; the right panel shows the bias:X where X is T_x, T_m, T_n, DTR. We show the mean and the standard error (SE)

$$SE = SD/\sqrt{N} \tag{3}$$

where SD is the standard deviation of the daily biases, and N is the number of days in that bin. The SE bars are small in Figure 1 because of the large sample size.

The left panel shows that the observed diurnal range increases almost linearly with decreasing opaque cloud cover, as T_x reaches a maximum under nearly clear skies and the minimum temperature T_n falls a little under clear skies. The reanalysis has a similar dependence, but the right panel shows that the biases in T_x, T_n and DTR in ERAI increase systematically as opaque cloud decreases. Under nearly clear skies, bias:T_n reaches +2°C, bias:T_x reaches −1.5°C; so that bias:T_m is small and positive, since it is close to the mean of bias:T_n and bias:T_x. However, these warm season 2 m temperature biases are of opposite sign for the daytime unstable boundary layer (BL) and night-time stable BL, so that bias:DTR reaches a remarkable −3.5°C under nearly clear skies.

Figure 2 shows the seasonal dependence of DTR in observations (left) and ERAI (right) from April to October. At low cloud cover, the observations have a higher DTR then ERAI in all months, consistent with the mean in Figure 1. In addition there are differences in the seasonal structure. In the observations DTR is largest in April and May and lowest in July, which is consistent with low evaporation in spring and high evaporation in mid-summer at the peak of crop growth. In the reanalysis, however, DTR falls substantially from April and May to October.

Figure 3 shows the seasonal cycle in the ERAI biases in DTR, its components T_n, T_x (top panels), and the corresponding mean T_m (bottom left). The negative bias of DTR (bottom right) changes little from April to July,

Table 2. Vegetation Representation in ERAI for the Grid Nearest to Climate Stations

Station Name	Low Vegetation Class	Low Vegetation Cover	High Vegetation Class	High Vegetation Cover	Bare Soil Cover
Regina	Crops/mixed farming	0.812	Deciduous broadleaf trees	0.088	0.100
Estevan	Crops/mixed farming	0.879	Interrupted forest	0.021	0.100
Prince Albert	Crops/mixed farming	0.704	Deciduous broadleaf trees	0.196	0.100
Saskatoon	Crops/mixed farming	0.897			0.103
The Pas	Crops/mixed farming	0.338	Evergreen needleleaf trees	0.562	0.100

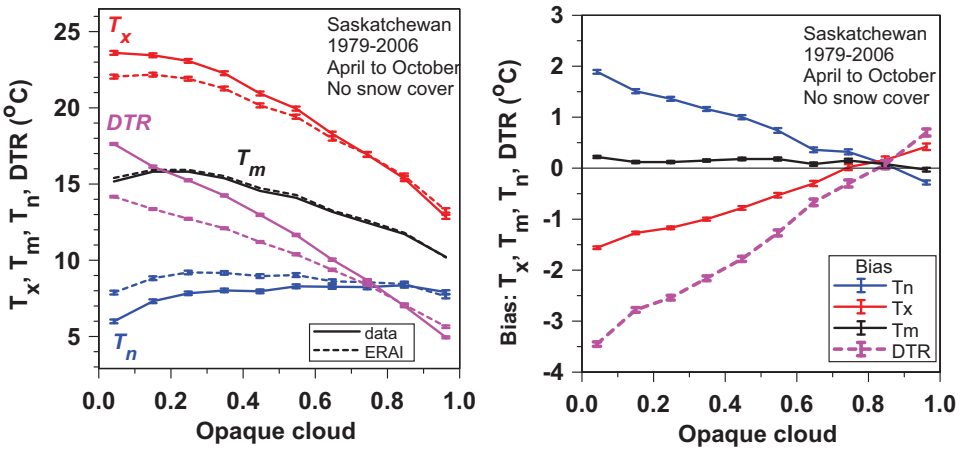


Figure 1. Opaque cloud dependence of T_n, T_m, T_x and DTR for (left) observations and ERAI and (right) corresponding ERAI biases in the warm season. The vertical bar represents standard error.

becomes larger negative from August to September, and reaches −5°C under clear skies in October. The warm bias in T_n increases almost monotonically from April to October. The cold bias in T_x changes less than does T_n: it is generally smaller in summer, when solar heating and evaporation are largest, than in spring and fall, when solar forcing is weaker. The climate bias in T_m increases from negative values in spring to positive values in fall. However this mean T_m bias is small: in April and May, ERAI underestimates the number of growing degree-days above 5°C by about 1%, and in September overestimates them by about 1%.

We see that the biases increase under clear skies, when the SW and LW fluxes, which drive the daytime unstable BL and night-time stable BL, are largest (and the cloud forcing is smallest). The seasonal trends of the stable BL biases in T_n and the unstable BL biases in T_x are quite distinct. This suggests it may be possible to link them to specific processes in the model surface and BL physics that couple land, BL and clouds (see section 6).

4.2. Prairie Cold Season Biases

We merged the same four stations in Saskatchewan to show the November to March cold season biases. We further selected only those days (12,465 days) when both ERAI and the climate station had surface snow cover, since snow cover has such a large impact on the surface coupling [*Betts et al.*, 2014a; *Betts and Tawfik*, 2016]. Figure 4 for the cold season shows a pattern of warm biases in ERAI, which under nearly clear skies reach +2.2°C for bias:T_n, +1.4°C for bias:T_x and +1.9 for bias:T_m. As a result bias:DTR is close to −0.9°C

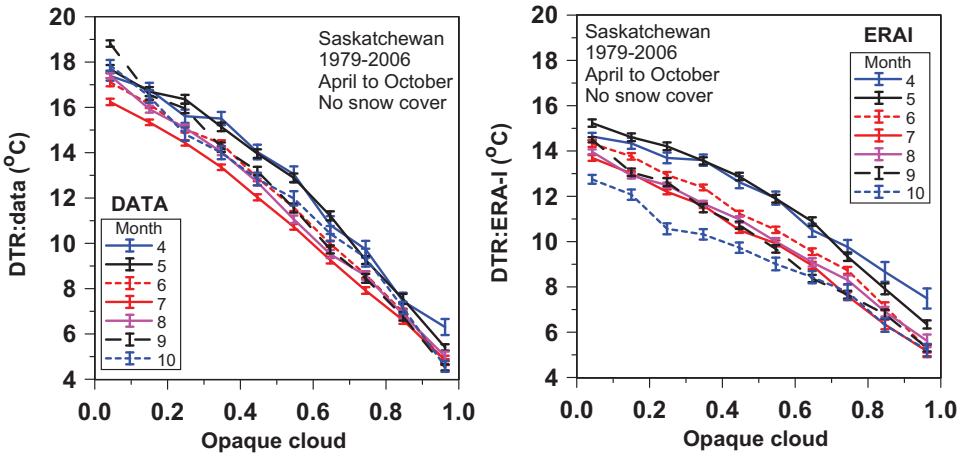


Figure 2. Opaque cloud dependence of monthly DTR for (left) observations and (right) ERAI.

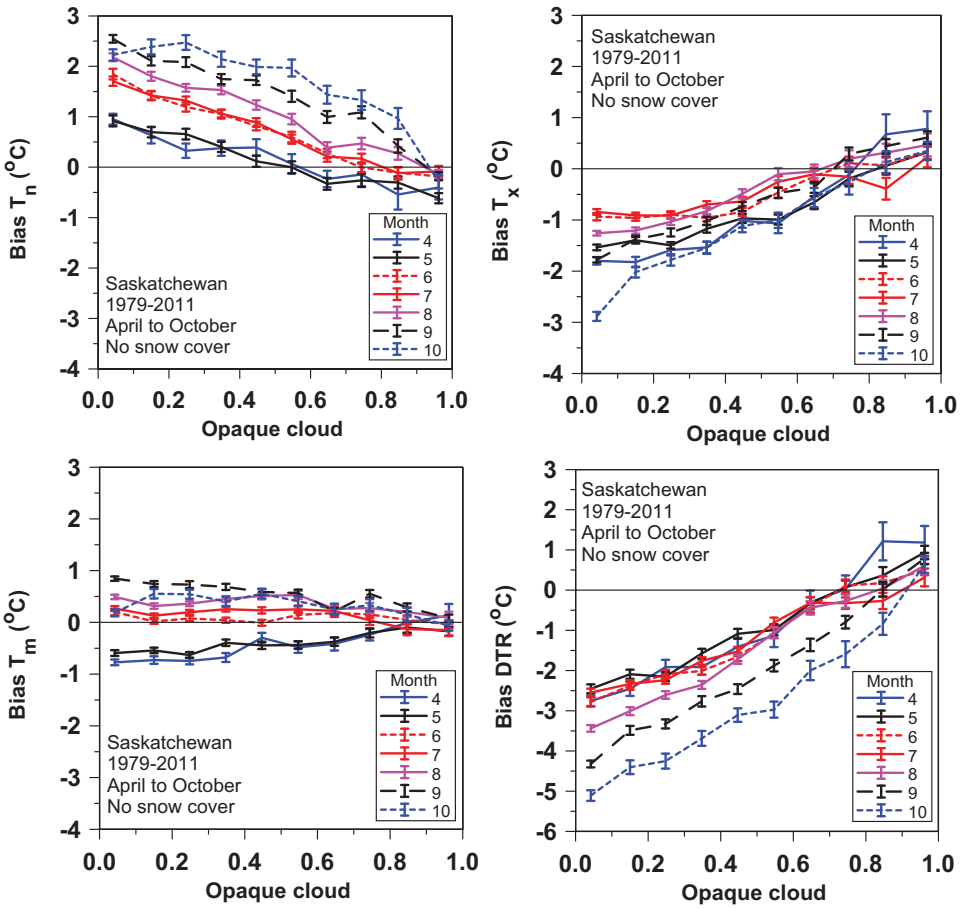


Figure 3. Opaque cloud dependence of monthly biases of T_n, T_x, T_m and DTR.

over most of the cloud cover range. These biases differ from Figure 1, with an opposite sign for T_x, perhaps because an unstable daytime BL is rarely established over snow in winter.

Figure 5 shows the monthly ERAI biases through the cold season for the four Prairie sites in Saskatchewan. The positive bias of T_n reaches +3°C in December and January under clear skies, but it falls to a low value in March. The smaller positive bias of T_x changes little through the cold season. Consequently the positive bias of T_m, which reaches +2.5°C in January, falls in March; and the bias of DTR which is most negative at the

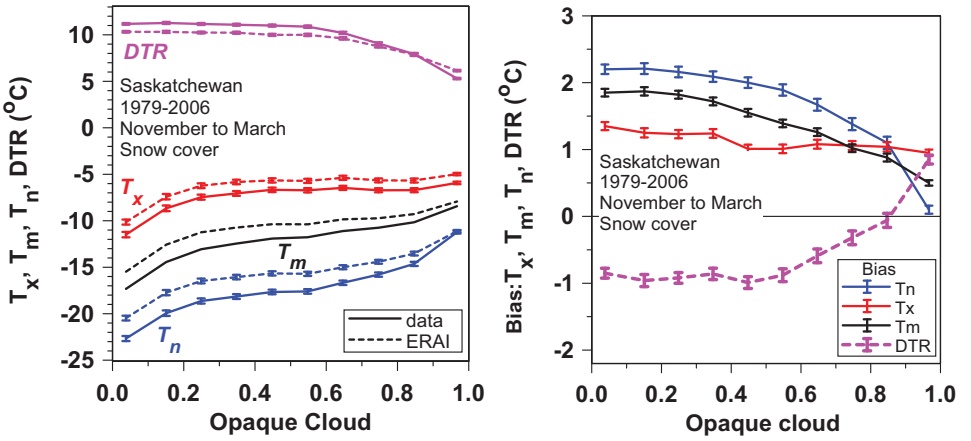


Figure 4. As Figure 1 for the cold season on Saskatchewan Prairies.

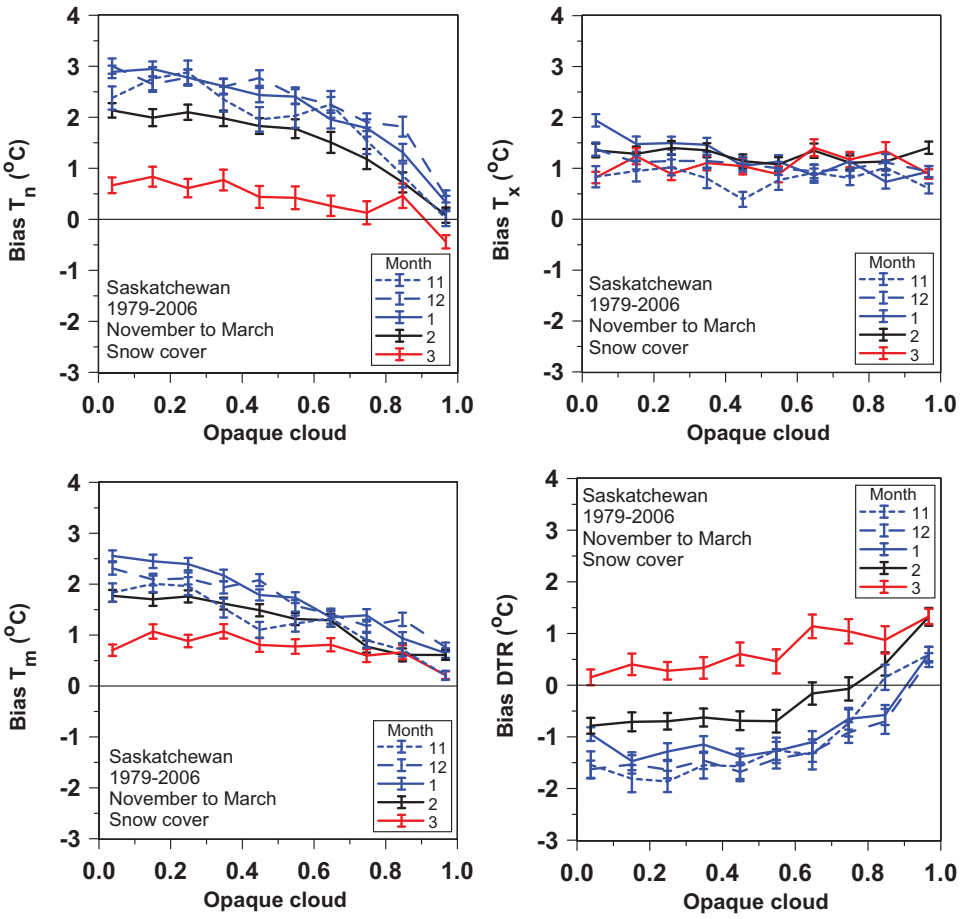


Figure 5. As Figure 3 for the cold season.

beginning of the cold season becomes positive by March. If we compare with Figure 3, we see there is little discontinuity in T_n across the snow transitions from March with snow to April without snow; and from October without snow to November with snow. However, for T_x there is a discontinuous change between positive biases in the cold season and negative biases in the warm season (see section 6.1 and Figure 9 later).

4.3. Wind-Speed Biases

Figure 6 shows the seasonal (left) and diurnal structure (right) of the wind-speed (WS) biases for the warm season (top) and cold season (bottom). The upper left panel for the warm season months shows the daily mean scalar wind-speed bias is negative in spring and very small in summer: there is little variation with daily mean opaque cloud cover. The lower left panel for the cold season shows a positive wind-speed bias that fall with increasing cloud. The right panels show diurnal variation of the wind-speed bias with daily mean opaque cloud cover is substantial especially in the warm season, and the diurnal amplitude increases with decreasing cloud cover.

It is believed that the momentum boundary layer at night is too diffusive in the reanalysis, which would reduce both the fall of near-surface wind-speed and temperature at night, giving a positive bias of both minimum temperature and wind-speed under clear skies. The negative wind-speed biases for the daytime unstable BL, suggest that the model may have too large a roughness parameter. However, there is uncertainty in the comparison, because the weather station measurements, which are usually located in open terrain, may not be representative of a grid box mean.

4.4. Biases in Downward Radiation

Figure 7 shows the ERAI biases in the downward shortwave and longwave fluxes as a function of opaque cloud cover for the warm and cold seasons. These were computed as the daily mean differences between

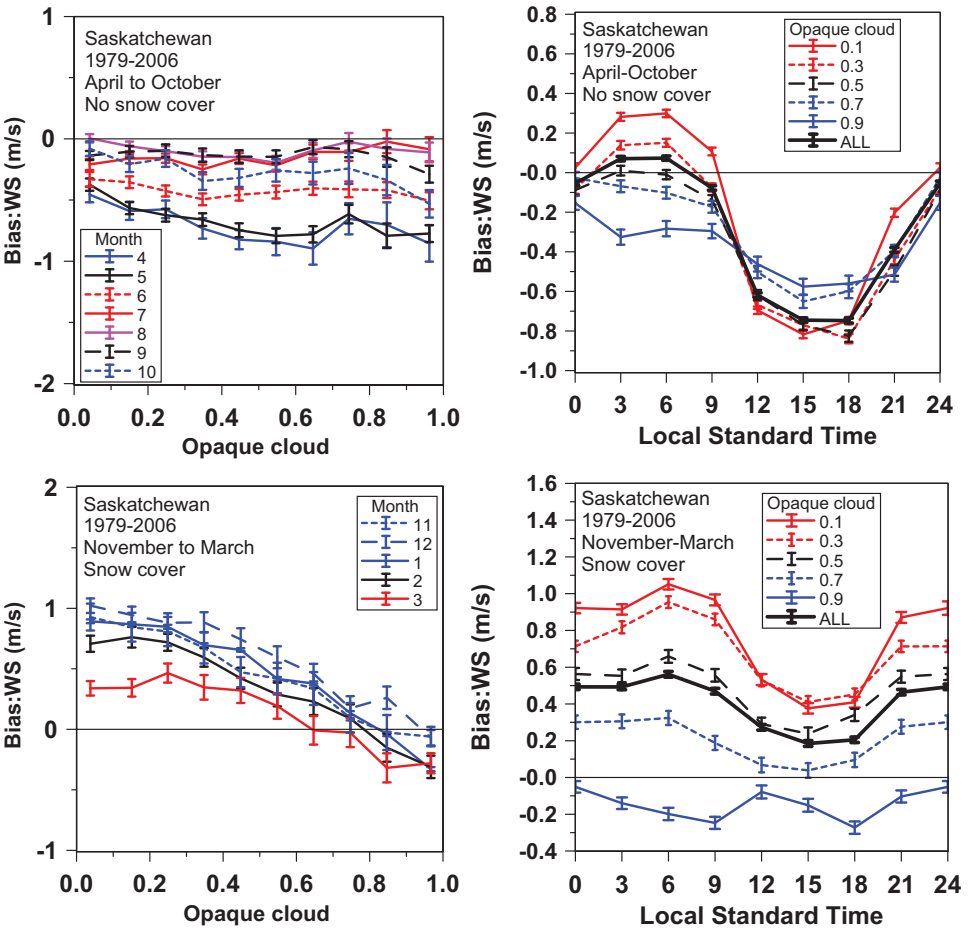


Figure 6. Opaque cloud dependence of monthly biases of (left) wind speed and (right) diurnal biases for (top) warm season and (bottom) cold season.

ERAI and the Bratt's Lake BSRN station data, which were used in *Betts et al.* [2015]. The stratification is by opaque cloud from Regina, which is 25 km north of Bratt's Lake: both are within the same ERAI grid-box. The bias:LW_{dn} is similar in warm and cold seasons, shifting from a small positive bias under clear skies to a small negative bias with cloudy conditions. The bias:SW_{dn} is small and negative in winter. In summer, the

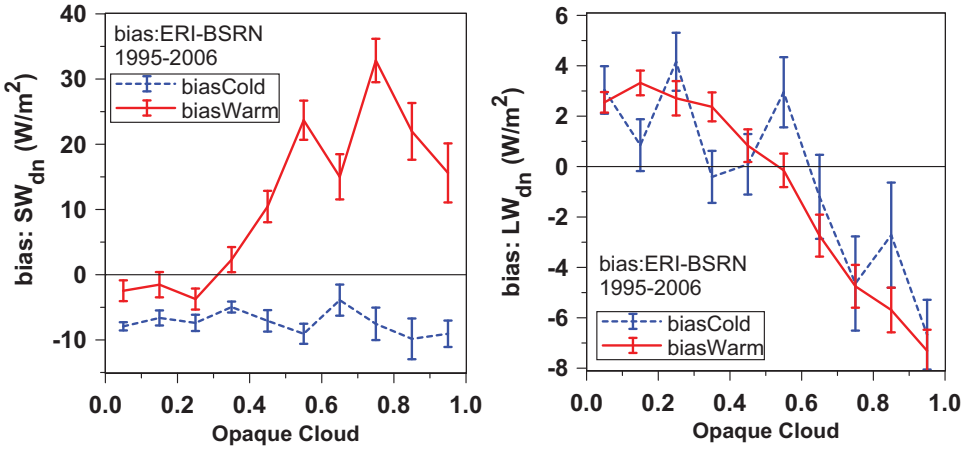


Figure 7. Biases in daily mean downward (left) shortwave and (right) longwave radiation for warm and cold seasons.

bias:SW_{dn} increases from a very small negative value under clear skies (seen in *Betts et al.* [2015]) to a significant positive bias as cloud cover increases, suggesting that the reanalysis cloud cover or cloud opacity is too small under these conditions. Because ERAI radiation biases are small at low cloud covers, it is unlikely that they are a primary cause of the temperature biases in Figures 1 and 3, which are largest under clear skies.

5. Boreal Forest Contrast

Section 3 shows composites from four Prairie stations in Saskatchewan. The ECMWF model has the tiled land-surface model discussed in section 2. The Prairies are represented in the model by the low vegetation types such as grassland and cropland; while to the north of the Prairies the boreal forest is modeled largely as high vegetation. Our data set contains a single boreal forest site at The Pas, Manitoba, which is roughly 310 km ENE of Prince Albert (Table 1), where the model grid-point fraction of tall vegetation is 0.562, modeled as evergreen needleleaf trees, while low vegetation fraction is 0.338, modeled as crops/mixed farming (see Table 2). Thus tall vegetation dominates this region. Because of the different tile physics, it is useful to contrast the reanalysis biases for the Prairie grid points dominated by low vegetation with the grid-point containing The Pas, which is dominated by the boreal forest.

Figure 8 shows the mean values for observations and reanalysis (left) and the bias of ERAI (right) for the warm season (top), for comparison with Figure 1, and the cold season (bottom), for comparison with Figure 4. The warm season biases for the boreal forest grid-point are much smaller than at the Prairie stations. Note that the scale has been enlarged. The bias:T_x is no longer negative under clear skies; and the T_n and DTR biases are much smaller. The variation with month is also much smaller than in Figure 3 (not shown). The cold season biases for this boreal forest grid-point (bottom panels) are similar to Figure 4 for the Prairies, but with a smaller spread in the warm biases for T_x and T_n so that the DTR bias is small.

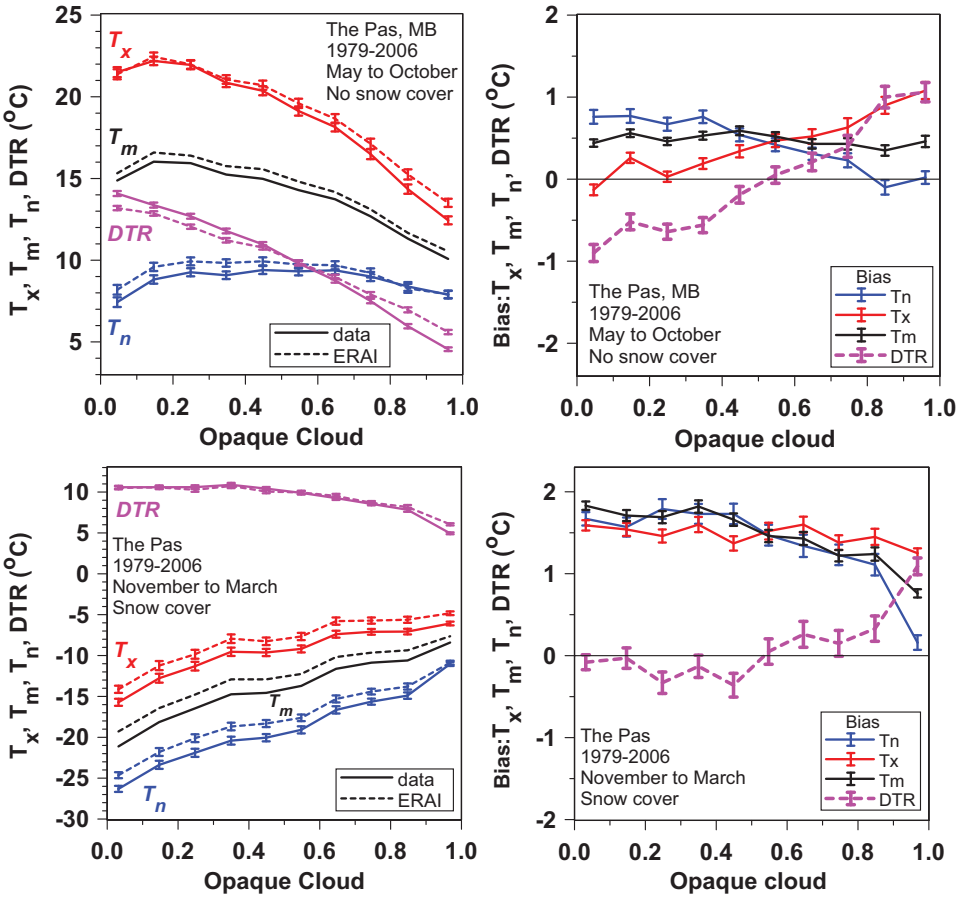


Figure 8. Warm and cold season biases for a boreal forest grid-point for The Pas for comparison with Figures 1 and 4.

So we see a sharp contrast between large biases for low vegetation (crops and grassland) with a large seasonal variation and generally smaller biases for tall vegetation (forests), especially in the warm season. In ERAI, tall vegetation has both a separate energy transfer model within the canopy and a separate model for the albedo of snow below the canopy [*Van den Hurk et al*., 2000]. The reduction in the warm season biases with a 56% forest cover in the model means the canopy model plays an important role. In the cold season, tall vegetation tiles have a far lower albedo, representing shaded snow under the canopy, than short vegetation where the snow covers the canopy, once it reaches a snow water equivalent of 15 mm. However this added complexity of the tall vegetation model means we do not attempt to interpret the boreal forest biases further. Instead we look further into the biases with the short vegetation model over the Prairies.

6. Discussion of ERA-Interim Diurnal Cycle Biases for the Prairies

The diurnal cycle biases over the Prairies, shown in Figure 3 and 5, have quite distinct seasonal trends in the warm and cold seasons. The biases are largest under clear skies, when the model SW and LW radiation biases are small (Figure 7), so we looked for possible causes in the surface energy budget and model land-surface parameters.

Unlike cropland, ERAI has fixed values of LAI which depend only on vegetation type. This lack of a seasonal variation is known to have an impact on seasonal temperature errors. Subsequent to ERAI, *Boussetta et al*. [2013] introduced an annual cycle of a satellite-derived monthly climatology of LAI, and found a marked improvement in temperature biases in the spring and fall transition seasons. Specifically reduced LAI in spring and fall, reduces evaporation and warms the surface temperature. Hence the lack of a seasonal cycle of LAI in ERAI is likely to produce cold daytime biases in spring and fall. The biases in wind-speed (Figure 6) are small and unlike the biases of temperature show little dependence on mean cloud cover.

The cold season composite in Figure 5 includes the presence of surface snow. ERAI has a single snow layer above the first soil layer with its own skin temperature and conductivity, which modifies the soil-atmosphere coupling. *Dutra et al*. [2010] have developed an improved snow model, which increases the snow thermal insulation as well as reducing soil freezing, leading to an improved hydrological cycle, but this revision postdates ERAI.

In the reanalysis the ground heat flux, G, in the warm season with no surface snow layer, satisfies the surface energy balance

$$G = R_{net} + SHF + LHF \tag{4}$$

where R_{net}, SHF, and LHF are the surface net radiation, sensible heat flux and latent heat flux, which are all defined positive downward. The ground heat flux in ERAI also satisfies the relation

$$G = \Lambda_{sk}(T_{sk} - ST1) \tag{5}$$

dependent on the difference between the skin temperature, T_{sk}, and the ERAI 0–7 cm soil layer temperature, ST1; and an empirical skin layer conductivity, $\Lambda_{sk}=10\ Wm^{-2}K^{-1}$ for low vegetation with no snow cover (see Table 7.2 of the model documentation [*ECMWF*, 2007]. There is an additional small direct radiative coupling to the first soil layer.

Snow uses the same formula (5), where ST1 is replace by the temperature of the single slab of snow and $\Lambda_{sk} = 7\ Wm^{-2}K^{-1}$. In this case Λ_{sk} represents the snow conductivity between the skin and the middle of the snow layer. The value is reasonable for thin snow layers but too large for thick layers, and therefore the thermal coupling between atmosphere and snow is too strong [*Dutra et al*., 2010]. The complete thermal coupling between atmosphere and soil also involves the heat diffusion between the snow pack and the soil. Here the heat conductivity is scaled with the thickness of the snow layer, and the insulation effect increases with deeper snow.

Possible biases in (4) that would lead to temperature biases are the lack of a seasonal cycle of LAI, which affects the seasonal partition between SHF and LHF; and strength of the soil-BL coupling, represented by Λ_{sk}, which affects the diurnal and seasonal amplitude of G.

6.1. Qualitative Discussion of the Diurnal Biases in Warm and Cold Seasons

We looked at the seasonal structure of the biases and surface energy balance under clear skies, defined as Opaque Cloud fraction < 0.1. Figure 9 (left) extracts the ERAI clear-sky seasonal cycle of the biases from Figures 3 and 5. We have replicated November and December so the winter cycle is clearly visible. The positive cold season biases in T_n, T_m and T_x are largest in mid-winter. The warm season composites from April to October are not continuous with the cold season composites from November to March, and the seasonal trends are quite distinct. The negative bias:T_x in the warm season and positive bias in the cold season gives a very large discontinuity across the snow-no snow boundary. In contrast bias:T_n is almost continuous across the spring and fall snow boundary, with a minimum in spring, rising to high values in mid-winter. However the large discontinuity in bias:T_x propagates to the corresponding discontinuities in bias:T_m and bias:DTR shown.

Figure 9 (right) show the corresponding terms in equation (4) in the monthly mean surface energy balance under clear skies, and the mean snow water equivalent, SWE in mm, for the ERAI surface snow layer. The surface energy balance is radically different between warm and cold seasons. Monthly mean SHF is positive (downward) for ERAI from November to February. This downward mean SHF, means that, unlike the warm season, there is a persistent stable BL which strengthens at night and weakens in the daytime. The downward shortwave flux is low around the winter solstice, because 60–70% is reflected by the high albedo of snow, which gives R_{net} negative from November to February [*Betts et al*., 2015], and only weakly positive in March. This is in sharp contrast to the warm season when monthly mean R_{net} reaches 189 W/m^2 in June under clear skies, and the strong solar heating drives an unstable daytime BL. Thus the reversal of the sign of bias:T_x between cold and warm seasons is associated with a shift from a stable to an unstable daytime BL; while the night-time stable BLs have warm biases throughout the year, with a minimum in spring and a maximum in December.

The Prairie climate stations in Saskatchewan have no measurements of the components of the surface energy balance, other than the BSRN measurements near Regina that were used to calculate the small biases in the downwelling radiation, shown in Figure 7. However, the positive bias:T_m under clear skies implies that the outgoing LW radiation in mid-winter is biased high by 8.5 W/m^2 with the mean January-February temperatures of 248 K. This heat loss is compensated by the sum of the upward flux G from the ground to the surface and the downward sensible heat flux, SHF, in the stable BL, since the latent heat flux LHF is very small (Figure 9, right).

It is believed that the momentum boundary layer at night is too diffusive in the reanalysis, which would reduce both the fall of near-surface wind-speed and temperature at night, giving a positive bias of both minimum temperature and wind-speed under clear skies (Figure 6). However, in the cold season there is very little variation in either windspeed (not shown) or wind-speed bias from November to February. So it likely that the seasonal variation in bias:T_n and bias:T_x which peak in mid-winter, when the soil is warmest

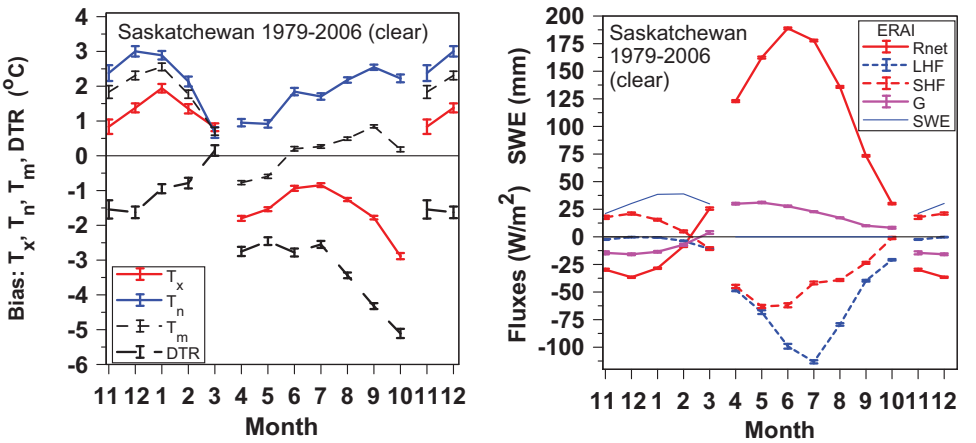


Figure 9. Seasonal cycle of clear-sky biases in (left) T_x, T_n, T_m and DTR and (right) seasonal cycle of clear-sky R_{net}, LH, SH, G and SWE in ERAI.

with respect to the skin temperature, is related to a positive bias in the upward ground flux G; while the difference between bias:T_x and bias:T_n is related to the diurnal cycle of the stable BL. This suggests that the seasonal amplitude of G may too large. This interpretation is consistent with experience by *Viterbo et al*. [1999] with an earlier model version. They found that winter bias and errors in night time cooling showed similarity and were pointing to the stable side of the atmosphere-surface coupling. They found that improvements could be made by adjusting the atmosphere turbulent diffusion and by adjusting parameters related to ground heat flux. So aspects of turbulent diffusion should not be excluded, although we feel that addressing ground heat flux issues has higher priority. Firm conclusions can only be drawn when more detailed information is available e.g., representative ground heat flux and accurate turbulent fluxes.

The warm season shows a radically different seasonal variation in the temperature biases. Bias:T_x reverses sign and becomes negative for the daytime unstable BL, which is driven by strong solar forcing and a large R_{net}. The small negative wind-speed biases, shown in Figure 6, for the daytime unstable BL, suggest that the model may have too large a roughness parameter, which would also bias:T_x negative. Mean G is largest in April when the soil is cool after winter, and smallest in October when the soil temperature is dropping after summer, but the air temperature is falling faster. Positive bias:T_n and negative bias:T_x is consistent with G being too large upward at night and too large downward in the daytime: which is consistent with Λ_{sk} being too large. Since the negative bias in DTR comes from the cold bias in T_x and the warm bias of T_n, it could be viewed as a consequence of a high bias in the diurnal amplitude of the ground heat flux in ERAI.

The seasonal dependence of bias:T_x from April to October has two possible causes: the lack of the seasonal dependence of LAI and the seasonal variation of G/R_{net}. Cropland has a ramp-up of LAI in spring and a fall of LAI after crop harvest and senescence in fall. Hence, fixed LAI will bias latent heat flux high and sensible heat flux low in spring and fall, giving larger negative bias:T_x in spring and fall. The impact of a downward daytime bias of G may also have a seasonal structure. For the 3 h data window at local noon, G/R_{net} in ERAI is smaller in summer (16%) than in spring (21%) and fall (23%). G/R_{net} being smallest in June is consistent with the negative bias:T_x being smallest in June.

The cause of the nearly monotonic increase in bias:T_n from April to October is less clear. It is possible that soil temperatures may have a cold bias in spring if there is an excess extraction of heat from the soil in winter, and a warm bias in fall if there is an excess storage of heat in the soil during summer.

Many issues cannot be resolved without quantitative sensitivity analyses and/or additional observations that can constrain the problem. We leave these for future work. The reanalysis is not only a fully coupled ground-BL-cloud-atmosphere system, there are also separate analysis temperature increments to both the atmosphere and the soil.

6.2. Comparison of Soil Heat Flux and Soil Temperatures at Lethbridge Prairie Site

We have no data at the Prairie climate stations on the soil temperatures or soil heat flux. However there is a FLUXNET-Canada research station near Lethbridge, Alberta at 49.43°N, 112.56°W, elevation 951m, over mixed grass prairie, measuring the soil temperatures at 2, 4, 8 and 16 cm and the components of the energy balance equation (4) [*Flanagan et al*., 2002; *Flanagan and Johnson*, 2005; *FLUXNET-Canada*, 2016].

Figure 10 compares the diurnal and seasonal cycle of the ground heat flux (left) and soil temperatures for June, July and August (JJA) for the coincident ERAI gridpoint and the Alberta grassland data (AB-GRL) for 5 years, 2003–2007, with the error bars showing the interannual variability (left). Figure 10 (top left) shows that the annual cycle of monthly mean ground heat flux in ERAI has roughly double the amplitude of the observations for this site. The soil heat flux is an average of values from two flux plates at 2 cm for 2003–2005 and four flux plates for 2006–2007. We made no correction for the thermal storage in the first 2 cm of soil. Note that the interannual variability in the reanalysis is large from January to March. The lower left panel shows the diurnal cycle comparison for the four seasons (December to February, DJF, March to May, MAM, June to August, JJA, and September to November, SON). We see that in all seasons, the amplitude of the diurnal cycle of the reanalysis ground heat flux is more than double that seen in these observations. Figure 10 (right) compares the mean JJA diurnal cycle of 2 m temperature and two soil temperatures. We show AB-GRL soil temperature at 4 cm, as a match for ERAI first soil layer, ST1, from 0 to 7 cm, and the AB-GRL

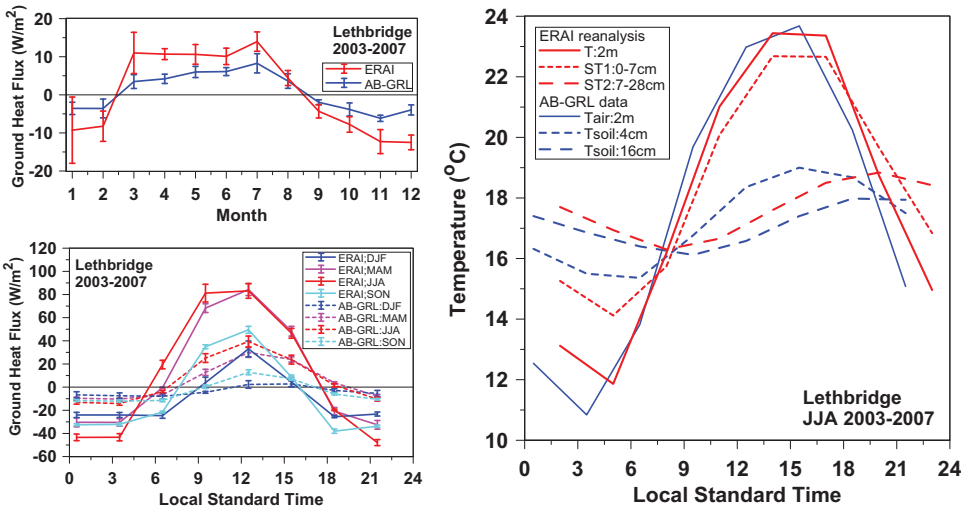


Figure 10. Comparison of the diurnal and seasonal cycle of (left) the ground heat flux and (right) soil temperatures for June, July and August (JJA) for ERAI and the Alberta grassland data (AB-GRL).

16 cm soil temperature as a match for the ERAI second soil layer, ST2, from 7 to 28 cm. While the 2 m temperatures have a similar mean diurnal cycle, the diurnal cycle of the soil temperatures has more than double the amplitude in the reanalysis than shown in the data. Both temperature and soil heat flux comparisons suggest much greater diurnal and seasonal exchange of heat with the soil in the reanalysis, or conceptually that the soil-atmosphere coupling in ERAI is much stronger than in these Prairie grassland observations. We are of course totally mismatched in scale. ERAI is a grid point mean, and the AB-GRL soil flux and soil temperature data are essentially point measurements for a grassland prairie site. However, consistency between soil heat flux data and the diurnal/seasonal evolution of temperature suggests that there is some realism in the data. The use of soil heat flux as a residual of atmospheric turbulent and radiative fluxes is not an alternative, because it is well known that the imbalance in surface energy budget observations is of the same order as the ground heat flux [*Oncley et al*., 2007]. In these Alberta grassland data, the April to August average daily surface energy imbalance is -38 W/m^2 (28% of R_{net}), much larger than the measured daily ground flux of 6 W/m^2. In models this energy balance is imposed, but it does not imply that errors in turbulent and radiative fluxes accumulate in the ground heat flux. The surface energy balance is part of the coupled system and surface skin temperature (which controls the ground heat flux) is highly interactive in models and in nature. The ERAI model has such strong interaction through the fast responding skin temperature, but also the simpler Penman-Monteith formulation for turbulent fluxes exemplifies strong interaction.

6.3. Linear Fits to the Growing Season Diurnal Biases

Figure 1 shows the mean warm season biases have a quasi-linear dependence on opaque cloud cover, but Figure 3 shows that the seasonal dependence is large, and also nonlinear for T_x and DTR. However the variation over the growing season, May to August (MJJA) is smaller than for April to October, so we derived linear fits to the mean MJJA biases as a function of mean opaque cloud cover ($OPAQ_m$). These could be useful as corrections in simple models. Bias:T_m is near zero, and the linear regression fits for T_x, T_n and DTR are

$$\text{Bias}: T_x = -1.41\ (\pm 0.18) + 0.176\ (\pm 0.010)\ OPAQ_m \left(R^2 = 0.97\right) \tag{6a}$$

$$\text{Bias}: T_n = 1.78\ (\pm 0.05) - 0.226\ (\pm 0.009)\ OPAQ_m \left(R^2 = 0.99\right) \tag{6b}$$

$$\text{Bias}: \text{DTR} = -3.19\ (\pm 0.08) + 0.402\ (\pm 0.014)\ OPAQ_m \left(R^2 = 0.99\right) \tag{6c}$$

Opaque cloud cover is an observed variable on the Prairies, not a model variable, and it could be argued that fits to a model variable such as R_{net} would be more useful. However simple linear fits are not suitable for R_{net}, because the dependence of monthly mean R_{net} on opaque cloud is nearly quadratic with the maximum under clear skies.

7. Conclusions

By comparing data from four climate stations on the Saskatchewan Prairies with corresponding grid-points in the ERAI reanalysis, we have explored the model biases in the mean diurnal cycle, represented by T_x, T_n, T_m and DTR, as a function of opaque cloud cover in the warm season without snow cover, and in the cold season with snow cover. Earlier work [*Betts et al*., 2013a; *Betts and Tawfik*, 2016] had shown that the diurnal temperature range is strongly dependent on diurnal and monthly timescales on opaque cloud, which determines the shortwave and longwave cloud forcing. *Betts et al*. [2014a] showed that reflective surface snow acts as a climate switch in the cold season and also reverses the sign of the net cloud forcing.

Our results in Figures 1–5 and 9 show that the model climate biases are quite distinct between the cold season with surface snow and the warm season (without surface snow). The warm season is characterized by an unstable daytime BL and a stable night-time BL; while the cold season with snow is dominated by a stable BL, both day and night.

The warm season biases increase as cloud cover decreases, and change substantially from April to October. Under clear skies, bias:T_x is negative of the order of -1°C in June and July, and -2°C in spring and fall; while bias:T_n increases almost monotonically from $+1$°C in spring to $+2.5$°C in October. Consequently bias:T_m increases from small negative values in April to small positive values in the fall, and bias:DTR falls under clear skies from -2.5°C in spring to -5°C in fall. These are substantial clear-sky biases when compared with the April to October 1981–2010 climate normals for Regina, for which mean DTR $=14$°C, and mean (T_x - T_m) $=7$°C.

The corresponding cold season biases have a very different structure. The primary difference is that bias:T_x is positive, of the order of $+1$°C, and varies little from November to March and with cloud cover. Both bias:T_m and bias:T_n are also positive in the cold season, reaching $+2.6$°C and $+3$°C respectively in January under clear skies. Both show a sharp fall in March as the solar zenith angle decreases. As a result the cold season bias:DTR increases from about -1.8°C in the fall to positive values in March.

The clear-sky ERAI temperature biases, summarized in Figure 9, have discontinuities in both spring and fall with the snow transitions. Bias:T_x has the largest discontinuity because it reverses sign from positive with the cold season stable BL to negative with the warm season unstable daytime BL. However, bias:T_n is quasi-continuous with a minimum in spring and a maximum in December. The result is that bias:T_m and bias:DTR have substantial discontinuities across the snow transitions.

We suggest that the ERAI diurnal cycle biases in 2 m temperature and their seasonal trends at these Prairie sites are consistent with a high bias in both the diurnal and seasonal amplitude of the model ground heat flux. For example, in the warm season the negative values of bias of T_x and the positive bias of T_n are consistent with the ground flux being too large downward in the daytime and too large upward at night. In the cold season stable BLs, the positive bias of T_n is largest in mid-winter when the soil-air temperature difference is largest. We also suggest that in the warm season, the lack of a seasonal cycle in the model leaf area index, gives too much evaporation in spring and fall, which contributes to a larger cold bias in T_x. However we recognize that in this fully coupled model system, biases in the formulation of both stable and unstable BLs may also contribute to the diurnal temperature biases.

Our evaluation of these model biases is only qualitative because although the Prairie climate stations have excellent hourly data for many decades, they have no measurements of the components of the surface energy budget, or of soil temperature that we can compare with reanalysis values. We used data from a BSRN site near Regina to show that the biases in the downwelling shortwave and longwave radiation fluxes in ERAI are very small under clear skies. To assess the ground flux coupling in ERAI, we compared soil flux and soil temperature data from a flux tower site (AB-GRL) over a grassland prairie near Lethbridge, Alberta with the corresponding grid point in ERAI. This comparison is totally mismatched in scale, since ERAI is a grid point mean, and the AB-GRL data are a mean of flux plates at 2 cm for 2003–2007. Nonetheless, this qualitative comparison suggests that the diurnal and seasonal amplitude of the ground fluxes in ERAI may be too large by a factor of the order of two.

We showed for comparison the ERAI biases for a boreal forest site with climate data at The Pas; and found that the model biases for a grid-point that had 56% tall vegetation were smaller in both warm and cold seasons than for the Prairie composite.

The identification of these reanalysis biases is of value for two reasons. The large model biases in the warm season are clearly important if reanalysis data are to be used for agricultural modeling, where our results can be used as bias corrections. Our methodology also provides targets for improving the model representation of the surface coupling for both daytime and night-time processes and over the annual cycle. This we leave for future work as it is not an easy task, because all aspects of the analysis-forecast system are involved. We will first assess how these biases have changed in ERA5, based on a more recent 2016 model version, *Dutra et al*. [2010] have already addressed reformulating the snow model to reduce the cold season biases, but the large warm season biases over short vegetation like the Prairie landscape need more study.

Acknowledgments
This work was partially supported by Agriculture-Canada, and NSF grant OIA 1556770 to the University of Vermont; and by ECMWF. We are very grateful to Larry Flanagan for the flux data set from Lethbridge, Alberta, and to the Canadian station observers who have made hourly climate observations for many decades. The Canadian Prairie data are available from the first author, or from Environment Canada at http://climate.weather.gc.ca/. The reanalysis data are available from ECMWF at https://ecmwf.int/en/research/climate-reanalysis/era-interim.

References

Beljaars, A. C. M., and P. Viterbo (1998), The role of the boundary layer in a numerical weather prediction model, in *Clear and Cloudy Boundary Layers*, edited by A. A. M. Holtslag and P. G. Duynkerke, pp. 287–304, Royal Netherlands Academy of Arts and Sciences, Amsterdam.

Betts, A., P. Viterbo, A. Beljaars, and B. J. J. M. Van den Hurk (2001), Impact of BOREAS on the ECMWF forecast model, *J. Geophys. Res.*, *106*, 33,593–33,604.

Betts A. K., and J. H. Ball (1997), Albedo over the boreal forest, *J. Geophys. Res.*, *102*, 28,901–28,910.

Betts, A. K., and A. B. Tawfik (2016), Annual climatology of the diurnal cycle on the Canadian Prairies, *Frontiers Earth Sci. 4*(1), doi:10.3389/feart.2016.00001.

Betts, A. K., R. Desjardins, and D. Worth (2013a), Cloud radiative forcing of the diurnal cycle climate of the Canadian Prairies, *J. Geophys. Res. Atmos.*, *118*, 8935–8953, doi:10.1002/jgrd.50593.

Betts, A. K., R. Desjardins, D. Worth, and D. Cerkowniak (2013b), Impact of land use change on the diurnal cycle climate of the Canadian Prairies, *J. Geophys. Res. Atmos.*, *118*, 11,996–12,011, doi:10.1002/2013JD020717.

Betts, A. K., R. Desjardins, D. Worth, S. Wang and J. Li (2014a), Coupling of winter climate transitions to snow and clouds over the Prairies, *J. Geophys. Res. Atmos.*, *119*, 1118–1139, doi:10.1002/2013JD021168.

Betts, A. K., R. Desjardins, D. Worth, and B. Beckage (2014b), Climate coupling between temperature, humidity, precipitation and cloud cover over the Canadian Prairies, *J. Geophys. Res. Atmos. 119*, 13,305–13,326, doi:10.1002/2014JD022511.

Betts, A. K., R. Desjardins, A. C. M. Beljaars and A. Tawfik (2015), Observational study of land-surface-cloud-atmosphere coupling on daily timescales, *Frontiers Earth Sci.*, *3*(13), doi:10.3389/feart.2015.00013.

Betts, A. K., R. Desjardins and D. Worth (2016), The impact of clouds, land use and snow cover on climate in the Canadian Prairies, *Adv. Sci. Res.*, *1*, 1–6, doi:10.5194/asr-1-1-2016.

Betts, A. K., A. B. Tawfik and R. L. Desjardins (2017), Revisiting hydrometeorology using cloud and climate observations, *J. Hydrometeorol.*, *18*, 939–955, doi:10.1175/JHM-D-16-0203.1.

Boussetta, S., G. Balsamo, A. Beljaars, T. Kral, and L. Jarlan (2013), Impact of a satellite-derived Leaf Area Index monthly climatology in a global Numerical Weather Prediction model, *Int. J. Remote Sens.*, *34*, 3520–3542.

Dee, D. P., et al. (2011), The ERA-Interim reanalysis: Configuration and performance of the data assimilation system, *Q. J. R. Meteorol. Soc.*, *137*, 553 - 597, doi:10.1002/qj.828.

Desjardins, R. L., S. N. Kulshreshtha, B. Junkins, W. Smith, B. Grant, and M. Boehm (2001), Canadian greenhouse gas mitigation options in agriculture, *Nutrient Cycling Agroecosystems*, *60*, 317–326.

Desjardins, R. L., W. Smith, B. Grant, C. Campbell, and R. Riznek (2005), Management strategies to sequester carbon in agricultural soils and mitigation greenhouse gas emissions, *Clim. Change*, *70*, 283–297.

Douville, H., J.-F. Royer, and J.-F. Mahfouf (1995), A new snow parameterization for the Meteo-France climate model, *Clim. Dyn.*, *12*, 21–35.

Douville, H., P. Viterbo, J.-F. Mahfouf, and A. Beljaars (2000), Evaluation of the optimum interpolation and nudging techniques for soil moisture analysis using FIFE data, *Mon. Weather Rev.*, *128*, 1733–1756.

Drusch, M., D. Vasiljevic, and P. Viterbo (2004), ECMWF's global snow analysis: Assessment and revision based on satellite observations, *J. Appl. Meteorol.*, *43*, 1282–1294.

Dutra, E., G. Balsamo, P. Viterbo, P. M. Miranda, A. Beljaars, C. Schär, and K. Elder (2010), An improved snow scheme for the ECMWF land surface model: Description and offline validation, *J. Hydrometeorol.*, *11*, 899–916.

ECMWF (2007), IFS documentation CY31R1, Part IV: Physical processes, ECMWF, Reading, U. K. [Available at https://www.ecmwf.int/en/forecasts/documentation-and-support/changes-ecmwf-model/ifs-documentation.]

Flanagan, L. B., and B. G. Johnson (2005), Interacting effects of temperature, soil moisture and plant biomass production on ecosystem respiration in a northern temperate grassland, *Agric. For. Meteorol.*, *130*, 237–253.

Flanagan, L. B., L. A. Wever, and P. J. Carlson (2002), Seasonal and interannual variation in carbon dioxide exchange and carbon balance in a northern temperate grassland, *Global Change Biol.*, *8*, 599–615.

FLUXNET-Canada (2016), *FLUXNET-Canada Research Network - Canadian Carbon Program Data Collection, 1993–2014*, ORNL DAAC, Oak Ridge, Tenn., doi:10.3334/ORNLDAAC/1335.

Haiden, T., M. Janousek, J. Bidlot, L. Ferranti, F. Prates, F. Vitart, P. Bauer, and D. S. Richardson (2016), Evaluation of ECMWF forecasts, including the 2016 resolution upgrade, *Tech. Memo. 792*, ECMWF, Reading, U. K. [Available at https://www.ecmwf.int/sites/default/files/elibrary/2016/16924-evaluation-ecmwf-forecasts-including-2016-resolution-upgrade.pdf.]

Holtslag, A. A. M., et al. (2013), Diurnal cycles of temperature and wind: A challenge for weather and climate models, *Bull. Am. Meteorol.*, *94*, 1691–1706.

Loveland, T. R., B. C. Reed, J. F. Brown, D. O. Ohlen, Z. Zhu, L. Youing and J. W. Merchant (2000), Development of a global land cover characteristics database and IGB6 DISCover from the 1 km AVHRR data, *Int. J. Remote Sens.*, *21*, 1303–1330.

Oncley, S. P., et al. (2007), The energy balance experiment EBEX-2000, Part I: Overview and energy balance, *Boundary Layer Meteorol.*, *123*, 1–28.

Smith, W. N., B. B. Grant, R. L. Desjardins, B. Qian, J. J. Hutchinson, and S. B. Gameda (2009), Potential impact of climate change on carbon in agricultural soils in Canada, 2000–2099, *Clim. Change*, *93*(3), 319–329.

Smith, W. N., B. B. Grant, R. L. Desjardins, R. Kröbel, B. Qian, D. E. Worth, B. G. McConkey, and C. F. Drury (2013), Assessing the effects of climate change on crop production and GHG emissions in Canada, *Agric. Ecosyst. Environ.*, *179*, 139–150, doi:10.1016/j.agee.2013.08.015.

Snauffer, A. M., W. W. Hsieh, and A. J. Cannon (2016), Comparison of gridded snow water equivalent products with in situ measurements in British Columbia, Canada, *J. Hydrol.*, *541*, 714–726.

Van den Hurk, B. J. J. M., P. Viterbo, A. C. M. Beljaars and A. K. Betts (2000), Offline validation of the ERA40 surface scheme, *ECMWF Tech Memo, 295*, 43 pp., ECMWF, Reading, U. K. [Available at https://www.ecmwf.int/en/elibrary/12900-offline-validation-era40-surface-scheme.]

Viterbo, P., A. C. M. Beljaars, J.-F. Mahfouf, and J. Teixeira (1999), The representation of soil moisture freezing and its impact on the stable boundary layer, *Q. J. R. Meteorol. Soc.*, *125*, 2401–2426.